Project funded by the Horizon 2020

Grant Agreement no. 829010

PRIME

Call: H2020-FETOPEN-2018-2020
Topic: FETOPEN-01-2018-2019-2020
Type of Action: RIA (Research and Innovation Action)
Name of Lead Beneficiary: CSIC, Spain
Project Start Date: 1st May 2019
Project Duration: 48-Months

DELIVERABLE 1.1:
First round of printable materials with photomechanical response

Due date of Deliverable:	30/04/2020
Actual Submission Date:	**29/04/2020**
Responsible partner:	TU/e
Report Author(s):	D.J. Mulder, S.J.D. Lugger, Zehra Kahveci, Carlos Sánchez-Somolinos
Type1[1]:	R
Dissemination Level[2]:	CO

[1] **Type**: Use one of the following codes (in consistence with the Description of the Action):
- R: Document, report (excluding the periodic and final reports)
- DEM: Demonstrator, pilot, prototype, plan designs
- DEC: Websites, patents filing, press & media actions, videos, etc.
- OTHER: Software, technical diagram, etc.

[2] **Dissemination level**: Use one of the following codes (in consistence with the Description of the Action)
- PU: Public, fully open, e.g. web
- CO: Confidential, restricted under conditions set out in the Model Grant Agreement
- CI: Classified, information as referred to in Commission Decision 2001/844/EC

DELIVERABLE D1.1: First round of printable materials with photomechanical response

TABLE OF CONTENTS

PRIME has received Funding from the European Union's Horizon 2020 research and innovation programme under Grant Agreement No. 829010

1 DOCUMENT HISTORY

Version	Date	Authors/ who took action	Comment	Modifications made by
0.1	16/04/2020	DMU and SL	First draft sent to CSS and ZK	
0.2	21/04/2020	CSS and ZK	Second draft sent to DMU	
0.3	23/04/2020	DMU	Third draft sent to PIs	
1.0	29/04/2020	CSS	Submitted to Commission	

Initials used:

DMU D.J. Mulder (TU/e)

SL S.J.D. Lugger (TU/e)

CSS Carlos Sánchez Somolinos (CSIC)

ZK Zehra Kahveci (CSIC)

PRIME has received Funding from the European Union's Horizon 2020 research and innovation programme under Grant Agreement No. 829010

2 LIST OF ABBREVIATIONS

3D	Three-dimensional
4D	Four-dimensional
AM	Additive manufacturing
Azo	Azobenzene
CSIC	Consejo Superior de Investigaciones Científicas
DIW	Direct Ink Writing
DSC	Differential scanning calorimetry
FFF	Fused filament fabrication
IPN	Interpenetrating network
LC	liquid crystal
LCE	liquid crystal elastomers
Me_2PPh	Dimethylphenylphosphine
NMR	Nuclear magnetic resonance
PVA	Polyvinylalcohol
TEA	Triethylamine
Tg	Glass transition temperature
THF	Tetrahydrofuran
TN-I	Nematic to isotropic transition temperature
TU/e	Eindhoven University of Technology
UV	Ultra-violet

PRIME has received Funding from the European Union's Horizon 2020 research and innovation programme under Grant Agreement No. 829010

3 DELIVERABLE DESCRIPTION AND SUMMARY

This deliverable report comprises the results of TU/e and CSIC on the design, synthesis, printing and characterization of an initial set of printable materials showing uniaxial alignment on printing and photoresponse.

The following three main objectives were set for the past reporting period:

1. Development of 4D printable photo responsive LCE inks considering the polymer chain nature and chemistry.
2. 4D Printing trails of LCE inks.
3. Characterization of 4D printed LCE photoactuators.

The first round of inks is based on thiol- and amine- acrylate oligomers containing azobenzene moieties as photoresponsive units. Three different thiol-acrylate oligomers were successfully prepared with different spacer length and regularity. By changing the spacers, the phase behaviour could be altered. Unfortunately, the inks based on thiol-acrylate oligomers have shown some instability issues upon longer storage. Using fresh inks within a week good results were obtained. But after longer storage, apparent cross-linking reactions occur. Also, two amine-acrylate oligomers were prepared having different molecular weights. However, the conditions for the aza-addition reaction were not optimal, leading to lower molecular weight oligomers than initially was aimed for. This led a deficient LCE network of some of the amine-acrylate inks probably due to the uncomplete crosslinking after photopolymerization. Still other amine-acrylate inks were prepared which led to useful materials for photoactuation.

Overall, the 3D printed samples showed good alignment before and after UV curing. Thermo actuation of the printed samples has been explored to get insight of the mechanical response and reversibility. Samples were typically contracted nearly half of their initial length after heating to 100 ºC and relaxed back to their initial size after cooled down. LCE samples prepared with one of the oligomers were not relaxed back to their initial size probably due to network formation issues in these samples. These samples were not contracted upon UV irradiation either. On contrary, samples prepared with the rest of the materials, the photoactuation studies have shown contractions up to 10% by UV light within the order of ten seconds of response time. The force measurements have shown that normalized force increases when illumination intensities increases. The increase of photoinitiator amount in ink formation increases the response to UV light in some of the studied materials.

For the next reporting period, a new set of oligomers will be prepared using optimized conditions. The molecular weight and the azo content will be varied to explore the effects of cross-link density and photo-thermal contributions. To reduce photo-thermal contributions and eliminate using harmful UV-light, fluoro-azobenzene chromophores will be synthesized and incorporated. Furthermore, new siloxane spacers have been designed and will be incorporated to lower the Tg and viscosity of the ink and elastomers. Lastly, thermoplastic LCEs will be evaluated either in their pure form or as semi-IPNs for improved processing and control over mechanical properties.

PRIME has received Funding from the European Union's Horizon 2020 research and innovation programme under Grant Agreement No. 829010

4 INTRODUCTION

In recent years, microfluidics has been becoming a growing market in many chemical and biological fields due to their reduced assay times and sample requirements which allows for handling valuable samples with a smaller footprint. Current developed technologies, however, are difficult to miniaturize which results in rather large off-chip equipment and requires careful operation thereof. The integration of active microfluidic functionalities such as valves, pumps, and mixers allow for the realization of small-scale and easy to operate microfluid devices that enable potential new applications and capabilities. Moreover, stimuli-responsive hydrogel-based fluidic components have been developed and implemented in microfluidic devices but rely on the absorption and release of water and show large response times which is unfeasible in fluidic devices.

Stimuli-responsive liquid crystal elastomers (LCE) are extensively being researched in combination with additive manufacturing (AM) techniques such as four-dimensional (4D) printing that allows for precise fabrication and programming of shape-morphing materials. Hence, this enables easy miniaturization and subsequent integration of reversible actuation functions in microfluidic devices that can be precisely controlled in a prescribed deformation. Implementing light-responsive properties in the microfluidic functionalities results in straightforward and remote operation of the device with a high temporal and spatial control of the response of actuation.

4.1 Objectives and approach

The aim is to design and develop 4D printable LCEs with a well-defined reversible photomechanical response and thereby considering the integration in microfluidic devices. Here, we conceptualized the implemented chemistry, polymer chain nature and molecular weight which ensures for optimization of the rheological and mechanical properties required for optimal additive manufacturing and mechanical response.

4.1.1 Design of LCE ink

Polymer chain nature

Looking at the types of LC polymers for photo responsive actuators available today, there are two main categories; (1) densely crosslinked liquid crystal networks and (2) loosely crosslinked liquid crystal elastomers (Table 1). Additionally, later in the project, an addition type (3) thermoplastic liquid crystalline elastomers will be introduced (See section 7 on page 29).

Table 1, Overview of responsive LC polymers.

(1) LIQUID CRYSTAL NETWORKS	(2) CROSSLINKED LIQUID CRYSTAL ELASTOMERS	(3) THERMOPLASTIC LIQUID CRYSTAL ELASTOMERS (FUTURE)
Glassy	Rubbery	Rubbery
High cross-link density	Low cross-link density	Physical cross-links (Crystalline or High Tg Blocks)
E = ~1-3 GPa	E = ~0.001 – 0.1 GPa	E = ~0.01 – 0.5 GPa
Poor rheological behaviour	Better rheological behaviour	Better rheological behaviour (higher T)
AM Method: Inkjet printing (from solution)	AM method: DIW	AM method: DIW or FFF

Densely crosslinked liquid crystalline networks with well-defined molecular orientation, can exhibit large macroscopic scale anisotropic mechanical response to different external stimuli. However,

PRIME has received Funding from the European Union's Horizon 2020 research and innovation programme under Grant Agreement No. 829010

the current dominant processing toolbox in liquid crystalline polymers is based on photo polymerization of low molecular weight monomers in a thin-film geometry. Typically, a glass cell with thickness in the range of microns provided with alignment layers is built and filled with reactive liquid crystalline monomers. After alignment is achieved, polymerization is triggered to create the aligned crosslinked morphology. Complex alignment layers with high degree of spatial control have been achieved using photoalignment technology however the complexity and size of the actuators is limited by the thin film geometry and the two orienting layers. Although, earlier works in literature showed that the material can be processed using inkjet printing, in the scope of the project, it does not lend itself to be 4D printed in more complex geometries by, for example, Direct Ink Writing (DIW). The low molecular weight monomers do not exhibit the required rheological characteristics and the obtained polymers are generally glassy in operation conditions.

To circumvent poor rheology and glassy materials, in our approach we will be focussing on using loosely crosslinked LCEs. Reactive LC oligomers having reactive groups at the chain termini are used as ink for AM. Using reactive oligomers instead of low molecular monomers leads to greatly enhanced rheological properties.[1–3] The mesogens can be incorporated in various manners into an LCE. They can either be built into the polymer backbone (main chain, **A**) or attached as pendant groups (side chain, **B**) (Table 2).[4]

Table 2, Backbone geometry of LCEs.[4]

(A) Main Chain	**(B) Side Chain**	
	Side-on	End-on
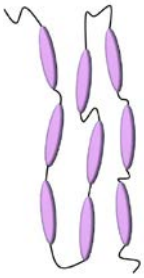		

During extrusion and deposition shear forces and/or elongational flow favour the alignment of the oligomer chains, building up orientational order of the mesogens along the needle moving direction. Therefore, the highest degree of orientation is expected to be achieved using a main-chain geometry **(A)**. This orientation enables a precise programming of the magnitude and directionality of the forces and therefore, well-defined reversible shape morphing of the 4D printed structures.

Nowadays, there is a large chemistry toolbox available for the fabrication of LCEs. The most reported methods are shown in Table 3. From the presented table, one can see that there are two main strategies to synthesize LCEs; **(1)** Click/addition chemistry and **(2)** hydrosilylation. LCE synthesis by hydrosilylation, however, requires a rather expensive metal complex as a catalyst and suffers from side reactions of which the impurities are hard to remove.[5,6] Moreover, via this reaction pathway only limit precursors are available that result in main-chain liquid crystal oligomers. In general, the latter **(1)** is most implemented in 4D printing applications due to the highly robust and efficient reaction pathway already under facile reaction conditions.[2,7,8] This

PRIME has received Funding from the European Union's Horizon 2020 research and innovation programme under Grant Agreement No. 829010

allows for great control over oligomer structure and molecular weight which are important factors in synthesizing stimuli-responsive actuators. Moreover, in click/addition reactions the mesogens are mostly arranged in the main chain which, as stated earlier, is preferred over side chain LCEs for improved programming and subsequent actuation thereof. Finally, the required LC precursors and chain extenders for these reactions are readily available or straightforward to synthesize which allows for flexible thermomechanical and physical properties of the LCE. Hence, the click/addition chemistry is much more preferred due to the more straightforward, cleaner and robust reaction and therefore the main chemistry in this project. Nevertheless, introducing siloxane moieties might be interesting due to the very low glass transition temperature (Tg) and viscosity of these blocks.

Table 3, The chemistry toolbox for LCE synthesis.[4]

(B) Side Chain	(2) Hydrosilylation	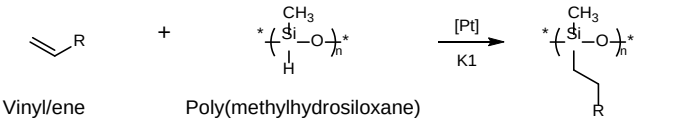	Vinyl/ene + Poly(methylhydrosiloxane) → [Pt], K1
		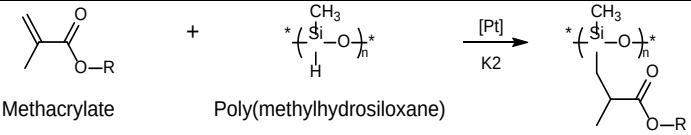	Methacrylate + Poly(methylhydrosiloxane) → [Pt], K2
(A) Main Chain		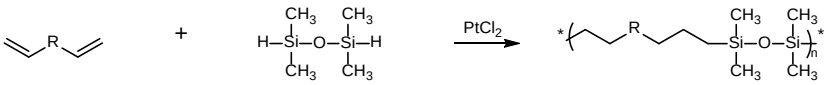	Diene + Tetramethyldisiloxane → $PtCl_2$
	(1) Click/Addition Chemistry	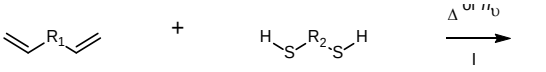	Diene + Dithiol → Δ or $h\upsilon$, I
		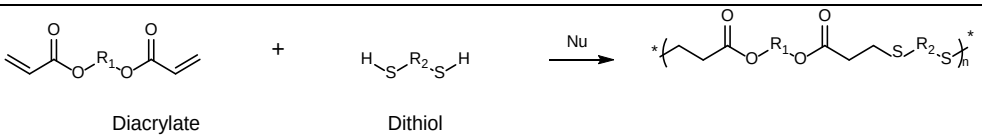	Diacrylate + Dithiol → Nu
		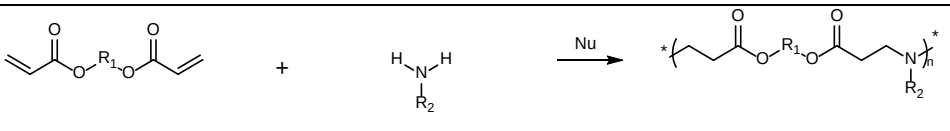	Diacrylate + 1° amine → Nu

PRIME has received Funding from the European Union's Horizon 2020 research and innovation programme under Grant Agreement No. 829010

Azo chromophores

In order to obtain a photomechanical response, a chromophore is required which can distort the molecular order of the mesogens in the LC matrix upon exposure to light.[9,10] Nowadays many photochromic compounds, *e.g*. azobenzene and spiropyran, have been incorporated in different systems to investigate the reversible light-driven isomerization reactions and their influence on present LC phases.[11] One of the most promising photochromophores is azobenzene and its derivatives, as shown in table 4, due to their similar rod-like shape in its *trans* isomer compared to the incorporated mesogens that can stabilize the LC phase. Moreover, the chemical structure of azobenzene derived compounds is like the LCs and easy to incorporate in the main chain. Illumination of these azobenzene chromophores yield bend shaped *cis* isomers which, unlike the *trans* isomer, distorts and destabilizes the LC phase.[12–15] Hence, this will reduce the molecular order of oriented mesogens in the LC phase and macroscopically change the dimensions of the material. The most common dialkoxy azobenzene has a rather slow thermal *cis-trans* isomerization with a lifetime of 1 day but requires ultra-violet (UV) light to be addressed. Fluorinated azobenzene derivatives are readily isomerized into its *cis* conformation by using visible light and thereby circumventing the use of UV.[16] Moreover, these fluorinated compounds have a very stable *cis* isomer with a lifetime up to 1 year and therefore a low photothermal effect. Alternatively, tautomerizing azobenzenes can also be addressed and isomerized by visible light but have a very fast isomerization reaction and short lifetime of 1 second which results in a very large photothermal contribution and subsequently heating of the material. Hence, the first round of printable materials with a photomechanical response will be realized with dialkoxy based moieties and later will be replaced by fluorinated derivatives to minimize the photothermal effect of the chromophore.

Table 4, Examples of common azobenzenes and their mechanism.

Dialkoxy azobenzene	Fluoro Azobenzene	Push-pull or Tautomerizing Azobenene
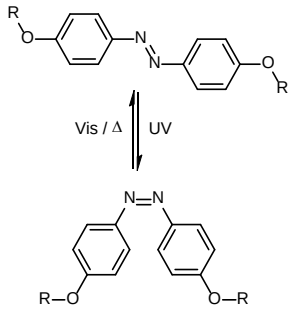	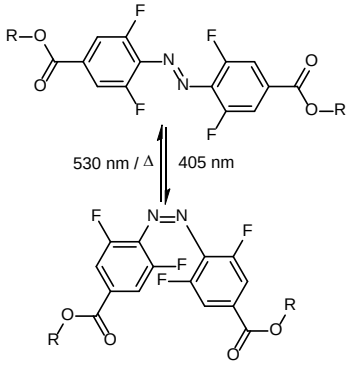	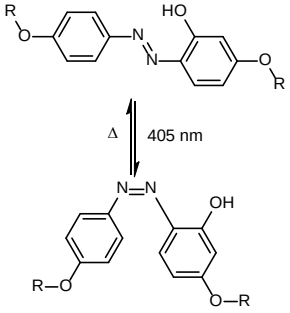

PRIME has received Funding from the European Union's Horizon 2020 research and innovation programme under Grant Agreement No. 829010

Molecular weight

The molecular weight of the LC oligomers can be easily controlled by altering the concentration of the precursors in the synthesis. This also allows for controllable viscosity of the reactive oligomers as it is directly proportional to the molecular weight which enables optimization of the mixture for 4D printing applications. Moreover, the induced alignment of the LC oligomers by shear and elongational flow is highly dependent on the rheological properties of the printed mixture. To obtain well defined and aligned printed shapes with high precision, the reactive LC oligomers should be processable by e.g. DIW and keep its shape after processing to be photo crosslinked into the final structure without modifications. Hence, the molecular weight of the mixture should be sufficiently high to obtain robust structures that are stable before crosslinking but still allow for printable materials. However, upon increasing the molecular weight of the LC oligomers the length between crosslinks increase and therefore the crosslink density in these materials decreases and its mechanical properties change. Moreover, this results in a decreased young's modulus as it is inversely proportional to molecular weight and gives a more flexible and elastic material. The viscosity of the printable LC mixtures and the mechanical properties of the obtained materials are highly dependent on the molecular weight of the synthesized LC oligomers. Hence, here this effect is conceptualized with respect to achieve optimal additive manufacturing and material properties.

4.1.2 4D printing and actuation

Additive manufacturing (AM) techniques enable the digital generation of material patterns in surfaces or fabrication of three-dimensional (3D) objects. 3D printing of conventional materials leads to immutable 3D objects with static shape, however 4D printing of responsive materials adds a 4th dimension as it leads to architectures that, with an appropriate stimulus such as heat, humidity, light, electric or magnetic fields, change their shape over time. As highlighted before, the use of responsive materials in combination with AM technologies enables the unique introduction of smart character to complex built structures that shift their shape in a preprogramed manner when exposed to the right stimuli. One of the hold-ups found in the further development of 4D printing, along with the conventional 3D printing technologies, is the lack of suitable materials presenting appropriate mechanical properties and response. Furthermore, robust methodologies are lacking to provide the structures with a controlled material morphology and therefore structure and function upon exposure to a trigger. Due to their large deformability, smart responsive polymers, mainly; shape memory polymers (SMPs), hydrogels and liquid crystalline elastomers (LCEs), are being widely investigated as the most remarkable candidate materials for 4D printing.

Liquid crystal elastomers have been exhaustively studied as stimuli responsive materials as they show large anisotropic mechanical actuation when exposed to a suitable trigger. LCEs with appropriate design show fast and reversible response to different stimuli including heat, light, moisture, pH or electrical fields. Actuation in these systems depends on the change of molecular order causing anisotropic stresses generated in the material. For instance, the temperature increase induces a decrease in LC order which leads to a contraction along the preferential direction of the LC molecules, the director **n**, and an expansion along the perpendicular direction. Thus, the precise control of the director allows the engineering of the mechanical response in these systems. Recently 4D printing of LCEs have been demonstrated.[1–3] As mentioned above, one of the first attempts to demonstrate this technique has made use of an ink comprising a main

PRIME has received Funding from the European Union's Horizon 2020 research and innovation programme under Grant Agreement No. 829010

chain liquid crystalline macromer which is functionalized with acrylate end groups. Extrusion-based printing is employed to deposit materials that are subsequently fixed through photopolymerization. By appropriately selecting the printing conditions (namely; material flux rate, deposition speed and nozzle diameter), alignment of the director can be attained after printing within the deposited filament (Figure 1a). This alignment is fixed through photo-induced polymerization precisely defining the director architecture of the printed structure. This morphology allows to digitally program stresses and deformations upon thermal stimulation (Figure 1b). Although the research groups that introduced the 4D printing of LCEs have used temperature as a trigger, other stimuli can be envisioned by appropriate design and synthesis of new printable materials with suitable printing and response characteristics.

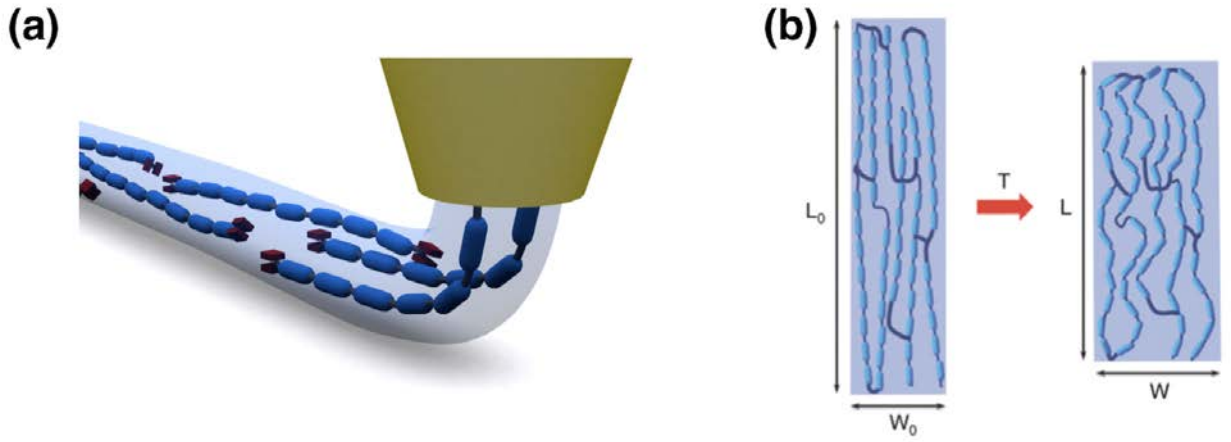

Figure 1, a) Imposed polymer main-chain alignment during the 3D printing. b) Thermomechanical response of uniaxially aligned LCEs.

PRIME aims to implement fluidic functions in microfluidic chips by using 4D printing of LCEs. Excitation of light responsive molecules incorporated in these systems introduces mesogenic disorder and therefore mechanical deformation of LCEs.[12–15,17] Crosslinked liquid crystalline polymers with well-defined molecular orientation, can exhibit large macroscopic scale anisotropic mechanical response to different external stimuli. In this way, no contact (pneumatic, electrical, mechanical) with the device will be required to implement mechanical functions and govern the microfluidic chip.

With the materials developed within the project, 4D printing parameters (material fluence, speed, nozzle geometry and diameter) will be optimized seeking for elements with optimum photo-deformation and work capacity. These studies will enable to select the best material candidates needed for integrated on-chip elements.

PRIME has received Funding from the European Union's Horizon 2020 research and innovation programme under Grant Agreement No. 829010

5 RESULTS

5.1 Synthesis of oligomers

5.1.1 Thiol-acrylate oligomers

A set of 3 different photoresponsive oligomers were prepared using thiol-acrylate click chemistry. For this a mixture of liquid crystalline diacrylates (**1-3**) –of which one contains a dialkoxy azobenzene moiety (**3**)– and a dithiol momomer (**4**) were used (Scheme 1).

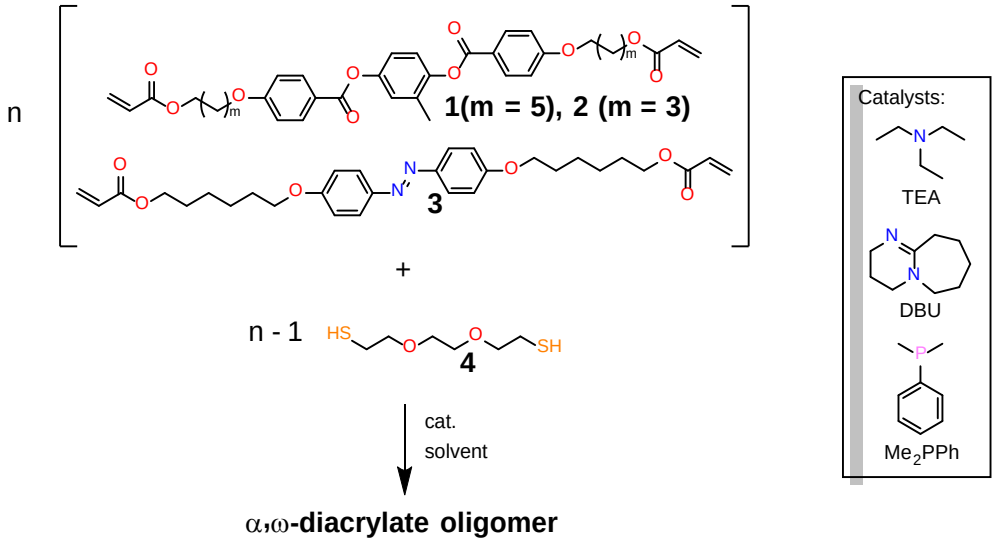

Scheme 1, Synthesis of thiol-acrylate monomers.

While the molecular weight of the oligomers was kept the same, the spacer length and regularity between the mesogens was varied by using either only monomer **1** (6 carbons) or **2** (3 carbons)**,** or a mixture or both **1** and **2** (irregular spacing). By varying the stoichiometry of the reactants, the molecular weight of the liquid crystalline oligomer is controlled. To obtain an α-ω-diacrylate oligomer, a substoichiometric amount of dithiol is used in the reaction. Typically, when large and regular spacers are used, crystallinity and smectic mesophases are obtained in the oligomers.[18] Reducing the length of the spacers will result in disappearance of crystallinity and formation of only a nematic mesophase. Besides the change in (meso)phase, a raise of the glass transition temperature is expected due to the net increase of aromaticy. Our hypothesis is, by using a combination of monomers with different length spacers, we can introduce an irregularity, giving a nematic mesophase while keeping the Tg low.

Liquid crystalline oligomers and elastomers based on thiol-acrylate click-chemistry are typically prepared using an organic base catalyst such as triethylamine (TEA). For the reaction to proceed smoothly, a 5-fold excess of this base is added.[19] Recent publications have shown, that when a more nucleophilic catalyst is used the reaction rate can be enhanced substantially. For example, when dimethylphenylphosphine (Me_2PPh) is used as catalyst, a concentration of less than 0,5 wt.% is sufficient.[20]

PRIME has received Funding from the European Union's Horizon 2020 research and innovation programme under Grant Agreement No. 829010

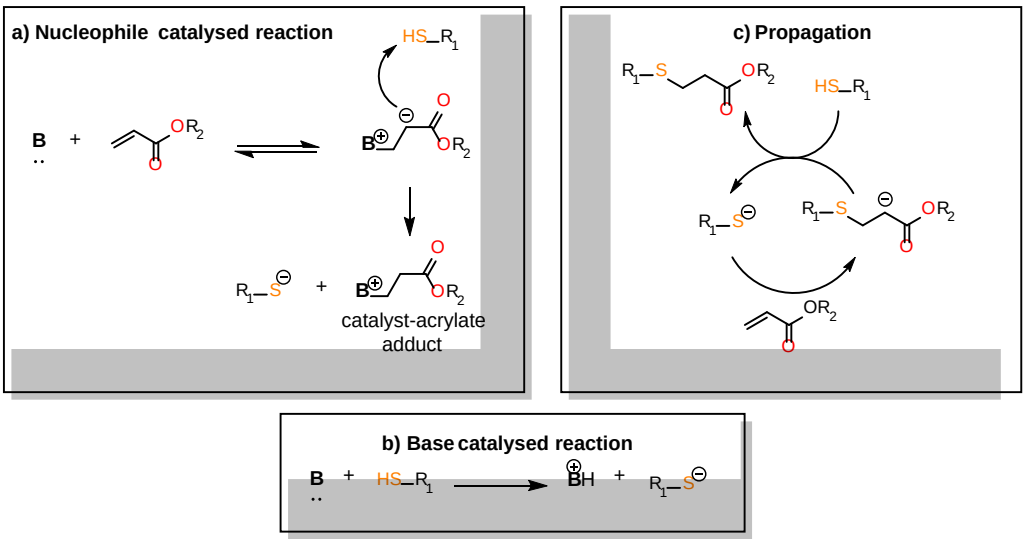

Figure 2, Reaction mechanism of thiol-acrylate addition. a) Nucleophile catalysed reaction, b) Base catalysed reaction, c) reaction propogation.

When comparing the new reaction conditions using 0,56-0.69 wt.% Me2PPh with the previous using 5 eq. TEA we see a great increment in reaction rate. The reaction was completed within 15 minutes at room temperature, where the TEA catalysed reaction was run overnight at a slightly elevated temperature (40 °C) to reach completion. The oligomer composition is given in Table 4:

Table 4, overview of the composition of the thiol-acrylate oligomers.

	Oligomer T1	**Oligomer T2**	**Oligomer T3**
1	4.6277 g	-	2.4378 g
2	-	4.5016 g	2.1317 g
3	0.1813 g	0.1812 g	0.1826 g
4	1.2099 g	1.3485 g	1.2726 g
Me_2PPh	0.034 g	0.042 g	0.037 g
TOTAL	6,0529 g	6,0733 g	6,0617 g
Solvent:			
DCM	12 mL	12 mL	12 mL
wt.% 3	3.0 %	3.0 %	3.0 %
wt.% Me_2PPh	0.56 %	0.69 %	0.61 %

PRIME has received Funding from the European Union's Horizon 2020 research and innovation programme under Grant Agreement No. 829010

Using the stoichiometric ratio (r) (Eq. (1)) and assuming full conversion (p = 1), a number-average degree of polymerization ($\bar{X}_n$) can be calculated (Eq. (2)). Subsequently, the number-average molecular weight (M_n) van be calculated using the molecular weight (M_i) and mol-fractions (x_i) of the individual monomers (Eq. (3)). The calculated values for the obtained oligomers can be found in Table 5.

$$\mathrm{r} = \frac{[\mathrm{dithiol}]}{[\mathrm{diacrylate}]} \quad \textbf{(1)}$$

$$\bar{X}_n = \frac{1+r}{1-r} \quad \text{(assuming p=1)} \quad \textbf{(2)}$$

$$M_n = \bar{X}_n \sum_i^n M_i x_i \quad \textbf{(3)}$$

The number-average molecular weight was determined by NMR. Using the integral of the protons on the benzoate phenyl ring (Figure 2, 4 protons, highlighted in orange) and the methyl substitute on the central phenyl ring (3 protons, highlighted in blue) of compounds **1** and **2** and the protons of the acrylate termini (6 protons, highlighted in green) the average number of repeating units can be calculated. The surface under the acrylate peaks was normalized at 6 to represent the average number of protons in the oligomer chain (Figure 3).

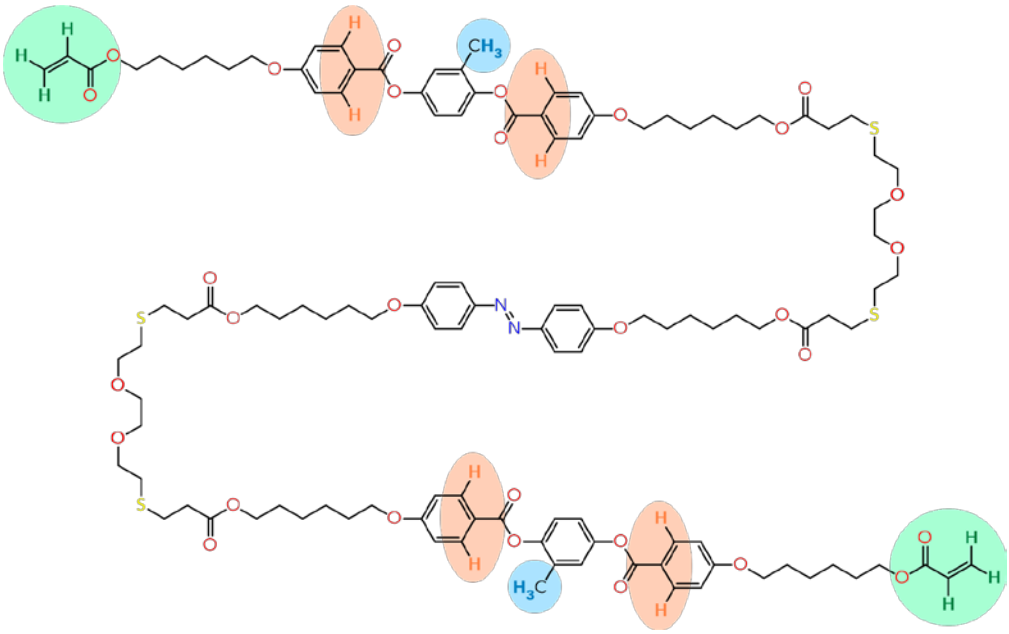

Figure 3, Representation of a short thiol-acrylate oligomer.

PRIME has received Funding from the European Union's Horizon 2020 research and innovation programme under Grant Agreement No. 829010

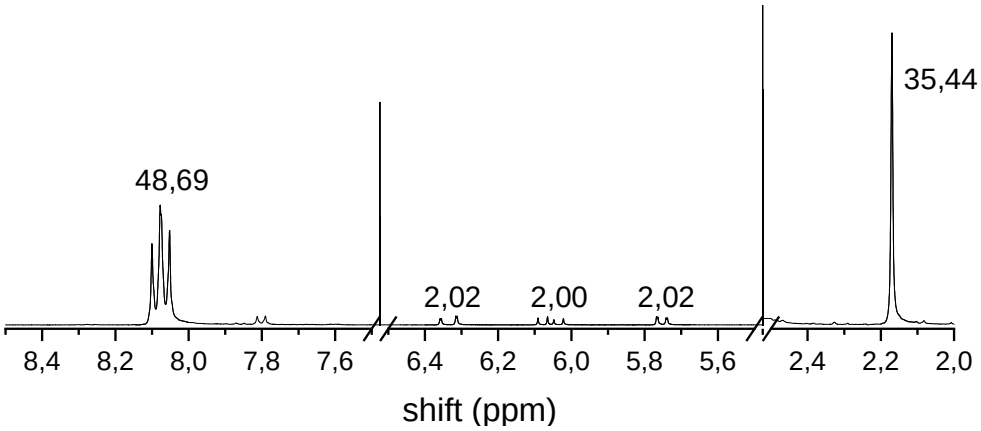

Figure 4, NMR spectrum of oligomer T1.

Using equation (4) and (5), the average number of repeating units was calculated. Since monomer **4** was not considered in the integral $I_{8.08ppm}$ or $I_{2.16ppm}$, a correction was applied. In this part of the equation y_i represents the mol-fraction of only acrylate bearing monomers.

$$n = \left(\frac{I_{8.08ppm}}{4\ protons} - 1\right)\frac{\sum_i^n y_i}{y_1 + y_2} \quad \textbf{(4)}$$

$$n = \left(\frac{I_{2.16ppm}}{3\ protons} - 1\right)\frac{\sum_i^n y_i}{y_1 + y_2} \quad \textbf{(5)}$$

The NMR results are summarized in Table 5 . The molecular weights of the obtained oligomers correspond well with the expected values.

Table 5, Overview of calculated r, X_n, n, and M_n, and experimental n and M_n for T-series oligomers.

Oligomer	r	Xn	n	Mn (g/mol)	n (NMR)	Mn (NMR) (g/mol)
T1	0.9185	23.551	11.275	10223	11.55	10464
T2	0.9253	23.764	12.282	10096	12.92	10517
T3	0.9210	24.315	11.657	10044	11.02	9517

PRIME has received Funding from the European Union's Horizon 2020 research and innovation programme under Grant Agreement No. 829010

Differential scanning calorimetry measurement were conducted (Table 6, Figure 4) to confirm our hypothesis that, by using a combination of monomers with different length spacers, we can introduce an irregularity, giving a nematic mesophase while keeping the Tg low. The experiments indeed showed an additional broad transition around 60 °C (heating) and 50 °C (cooling) in sample **T1** which might indicate crystallinity. Furthermore, contrary to oligomers **T2** and **T3**, this oligomer solidifies upon standing which also suggest crystallinity. Looking at the glass transition temperature, a difference of 5 °C is observed between the oligomer with a 6-carbon spacer (**T1**) and 3-carbon spacer (**T2**). The Tg of the oligomer containing a mixture of monomers having 3- and 6-carbon spacers (**T3**) lies in-between the values of **T1** and **T2** at -16.6 °C / -20.2 °C (heating/cooling).

Table 6, overview of transition temperatures of T-series oligomers.

Oligomer	Tg (Heating/Cooling)	Ti (Heating / Cooling)
T1	-22.3 °C / -25.3 °C	82.0 °C / 80.9 °C
T2	-16.6 °C / -20.2 °C	57.1 °C / 52.7 °C
T3	-19.8 °C / -24.0 °C	71.4 °C / 70.4 °C

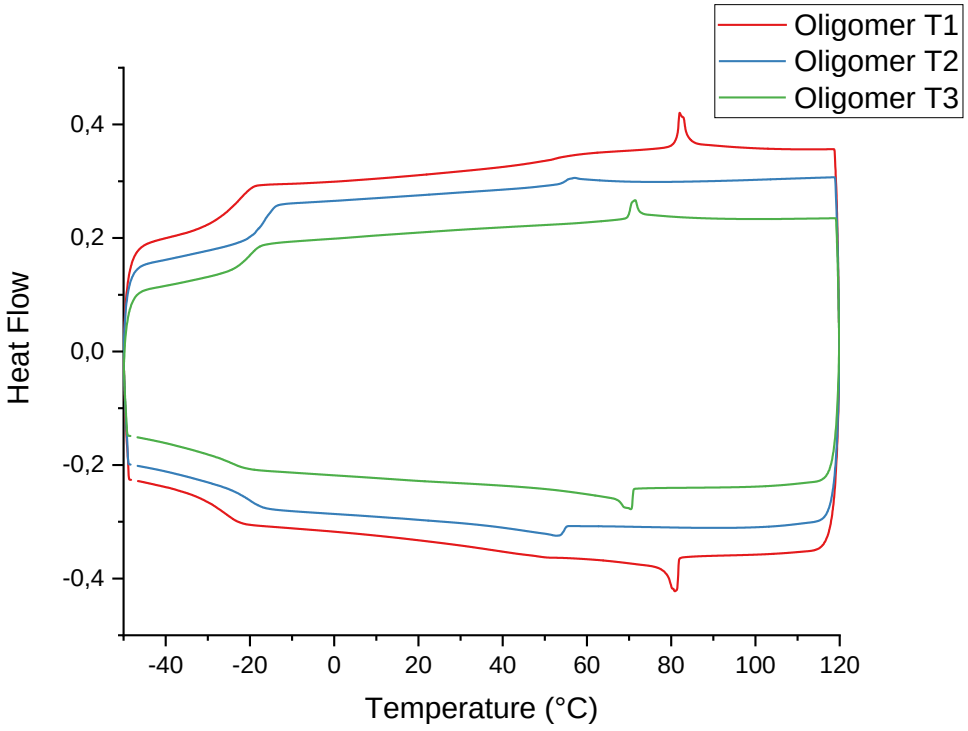

Figure 5, DSC traces of T-series oligomers.

PRIME has received Funding from the European Union's Horizon 2020 research and innovation programme under Grant Agreement No. 829010

5.1.2 Amine-acrylate oligomers

Two photoresponsive oligomers were prepared using amine-acylate aza-addition chemistry. The aza-addition is a self-catalysed reaction that typically is performed at elevated temperature (60 - 110 °C) in solution or bulk (Scheme 2).[1,2,21]

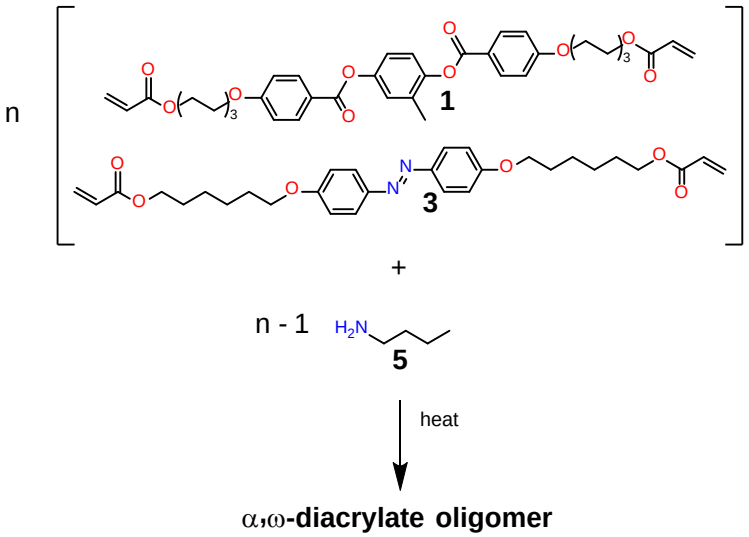

Scheme 2, synthesis of amine-acrylate oligomers

In our experiments we tried to vary the molecular weight of the oligomers. Oligomer **A1** was prepared using equimolar amount of both the amine and acrylate. Oligomer **A2** was prepared using an excess of acrylate to obtain an α-ω-diacrylate oligomer. The oligomers were prepared by dissolving compounds **1**, **3** and **5** in THF and allowing the reaction to proceed at 80 °C for 20 hours in an open flask. After 20 hours, the oligomers were dried *in vacuo* at 80 °C for 6 hours. The composition of the oligomers can be found in Table 7.

Table 7, overview of the composition of the amine-acrylate oligomers.

	Oligomer A1	**Oligomer A2**
1	5.239 g	5.279 g
3	0.178 g	0.181 g
5	0.595 g	0.551 g
TOTAL	6,012 g	6.010 g
Solvent:		
THF	12 mL	12 mL
wt.% 3	3.0 %	3.0 %

PRIME has received Funding from the European Union's Horizon 2020 research and innovation programme under Grant Agreement No. 829010

Like the thio-acrylate oligomers, also here we determined the number average molecular weight by NMR. The same signals and equations could be used for the calculation. As example, the spectrum of oligomer **A1** is shown in Figure 5.

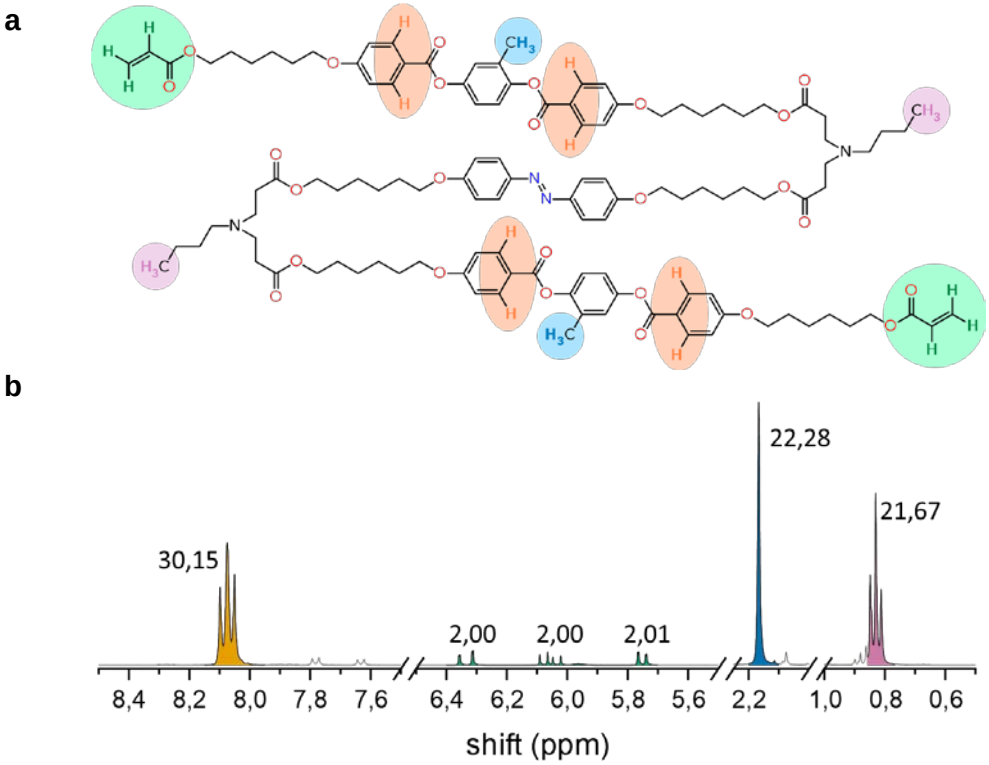

Figure 6, NMR characterization of A-series oligomers. a) Representation of a short thiol-acrylate oligomer. b) NMR spectrum of oligomer A1.

The calculated and measured values are depicted in Table 8 . The obtained molecular weight of the oligomers was substantial lower than the aimed values. For oligomer **A1**, where equimolar amounts of the monomers were used, a molecular weight of only 5376 g/mol was obtained. This is most possibly caused by incomplete reaction due the reaction conditions used. The aza-addition reaction occurs in two steps with different reaction rates. In the first step a primary amine reacts with an acrylate to yield a secondary amine. Next, in the formed secondary amine reacts further with another acrylate to yield the final tertiary amine. Generally, this first reaction proceeds reasonable fast. The second step, however, proceeds at a much lower rate.[22] As a result, an incomplete reaction would end up in a mixture of both acrylate and sec-amine end-groups. This latter is confirmed by the integral of the terminal -CH_3 group (0.82 ppm) of the *n*-butylamine. For an n of 6.77 one would expect an integral of 20.31 (3 protons), but 21.67 was obtained instead, indicating the presence of residual amines either as free primary-amines or terminal sec-amines.

PRIME has received Funding from the European Union's Horizon 2020 research and innovation programme under Grant Agreement No. 829010

Table 8, Overview of calculated r, X_n, n, and M_n, and experimental n and M_n for A-series oligomers.

Oligomer	r	Xn	n	Mn (g/mol)	n (NMR)	Mn (NMR) (g/mol)
A1	0.9997	5791.5	2895	2141436	6.77	5376
A2	0.9191	23.7	11.4	9067	4.45	3785

Despite of the lower molecular weight, differential scanning calorimetry measurements were conducted on the amine-acrylate oligomers (Figure 6). From the both synthesized oligomers, oligomer **A1** showed slightly higher Tg and T_i than **A2** which might be related to the molecular weight. Oligomer **A1** has a Tg of -18 °C (heating) and a T_i of 88 °C (heating). Oligomer **A2** has a Tg of -21 °C (heating) and a T_i of 85 °C (heating). An overview of the transitions can be found in Table 9.

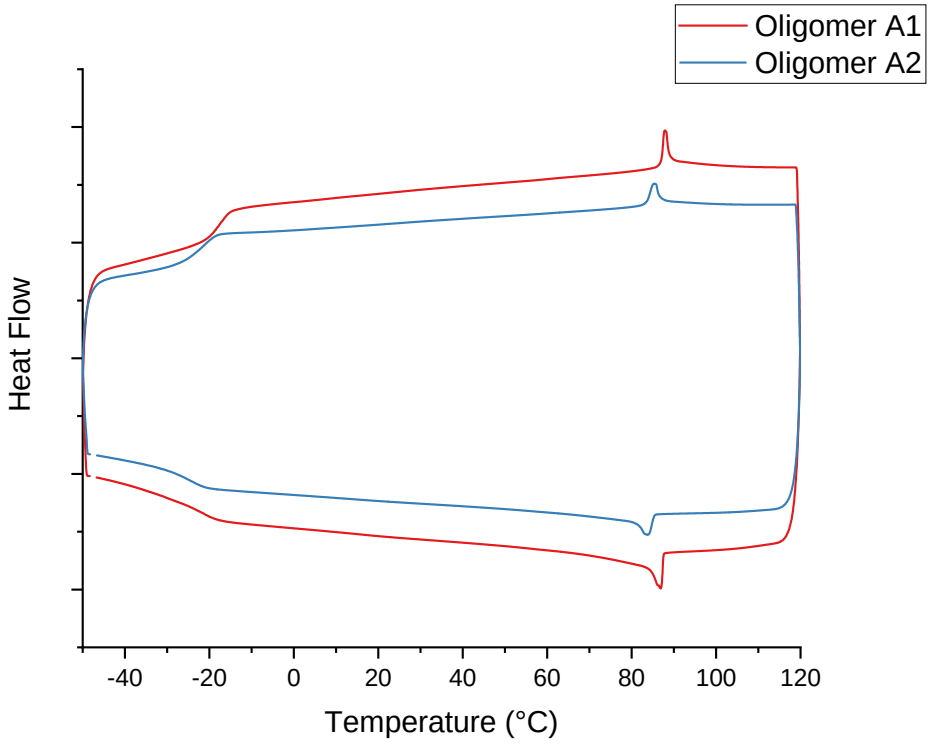

Figure 7, DSC traces of A-series oligomers.

Table 9, Overview of transition temperatures of A-series oligomers.

Oligomer	Tg (Heating/Cooling)	Ti (Heating / Cooling)
A1	-17.9 °C / -21.0 °C	87.9 °C / 86.9 °C
A2	-21.0 °C / -25.0 °C	85.4 °C / 83.5 °C

PRIME has received Funding from the European Union's Horizon 2020 research and innovation programme under Grant Agreement No. 829010

5.2 4D printing and actuation

5.2.1 Ink Preparation

Thiol (**T1**, **T2**, **T3**) and amine-acrylate (**A1**, **A2**) oligomers prepared by TU/e have been used to prepare photoresponsive inks. Besides, the amine-acrylate oligomer (**AA-12**), previously prepared at CSIC, was also incorporated to this study. **AA-12** was synthesized following a similar protocol as that described in section 5.1.2 and using the diacrylate **1**, and N-butylamine **5**, together with an azobenzene A9A homologous to **3** but having a flexible spacer of 9 carbon atoms. These compounds were added into a flask with a 1 : 1: 0.12 molar ratio.

Inks were prepared by mixing 1 gr of each oligomer, based on Thiol-acrylate and amine-acrylate chemistry, with 2 wt % of a visible photoinitiator, Bis(cyclopenta-1,3-diene)bis(1-(2,4-difluorophenyl)-3H-pyrrol-3-yl)titanium also known as IRGACURE 784, dissolved in tetrahydrofuran (THF) (approx. 1 gr). **AA-12** oligomer was also prepared by mixing 3,5 wt % of the photoinitiator IRGACURE 784, dissolved in THF (approx. 1gr). Mixtures were left mixing on a hot plate at 70 ºC for 72 h under extraction. Later, the solvent-free, viscous inks are transferred into the printing syringe and placed on to an extrusion-based 3D printer.

5.2.2 Optimization of printing parameters and LCE formation

We have first carried out the optimization of the printing conditions and 3D printing of these inks. Printing parameters have been explored seeking optimum printing conditions by studying aspects such as printing temperature, nozzle diameter, pressure and velocity for an optimal alignment. We have typically chosen printing temperature for inks that is below the nematic to isotropic transition temperature (T_{N-I}) and within the nematic regime. We start to explore the optimum printing temperature between 60 to 70 ºC within the nematic phase temperature range avoiding higher temperatures that could trigger undesired thermally induced polymerization for all inks. The nozzle diameter is another parameter that can affect the printing and alignment. A smaller nozzle diameter can allow higher resolutions while it requires higher printing pressure. Higher shear forces can affect molecular orientation in the interior of the needle. On the contrary, lower printing pressure can be applied at larger nozzle diameters resulting in effective molecular orientation after printing. Nozzle diameters in the range of 0.25-0.61 mm were explored. For fixed flow of material through the needle, changes in the printing velocity are explored as a further optimization parameter as it can also affect alignment due to elongational flow. This multivariable space has been globally explored for each ink seeking for adequate printing conditions leading to aligned samples.

Printing is performed with the optimal parameters on a Polyvinylalcohol (PVA) coated glass slide and the formation of monolithically aligned samples is checked. 3D printing of continuous stripes of deposited ink with uniaxial orientation is obtained by printing closely packed parallel lines along one direction. Birefringence of deposited ink is observed under the microscope between crossed polarizers. When the direction of the extrusion is parallel to the polarizer the printed line is dark, and when the molecular orientation is 45 º to the polarizer the printed line is bright (Figure 8). The resulting printed lines are subsequently fixed by photo-exposure. This photopolymerization leads to crosslinked elastomer formation. The anisotropic characteristic of printed samples is explored again after curing using the polarization microscope.

PRIME has received Funding from the European Union's Horizon 2020 research and innovation programme under Grant Agreement No. 829010

Thiol-acrylate inks

Thiol-acrylate inks were named **T1-IRG784-2**, **T2-IRG784-2** and **T3-IRG784-2** with the first part of the code referring to the oligomer **T1**, **T2** and **T3**, employed, **IRG784** referring to the photoinititiator and the last number at the end of the code, **2**, goes for to the percentage in weight of photoinitiator employed. Figure 8 shows the observed birefringence of a deposited line of ink between crossed polarizers, printed at range of 60-70 ºC. Larger nozzle diameter in the range of 0.41-0.61 mm were used to print **T2-IRG784-2** and **T3-IRG784-2**. We also identified an optimal flow of the material, while keeping the appropriate alignment for the 3D printing, with 5-6 bars for all inks.

Amine-acrylate inks

Amine-acrylate inks were named **A1-IRG784-2**, **A2-IRG784-2**, **AA-12-IRG784-2** and **AA-12-IRG784-3,5** with the first part of the code referring to the oligomer A1, A2 and AA-12 employed, **IRG784** referring to the photoinititiator and the last number at the end of the code, **2** and **3,5,** referring to the percentage in weight of photoinitiator employed. We explored printing temperatures between 60 to 65 ºC within the nematic phase temperature range avoiding higher temperatures that could trigger undesired thermally induced polymerization. Figure 8 shows the observed birefringence of a deposited line of ink between crossed polarizers. The nozzle diameter of 0.33 mm is used to print **A1-IRG784-2**, and **AA-12-IRG784-2** and it is decreased to 0.25 mm to print **A2-IRG784-2**. We identified an optimal flow of the material, while keeping the appropriate alignment for the 3D printing, with 4-5 bars.

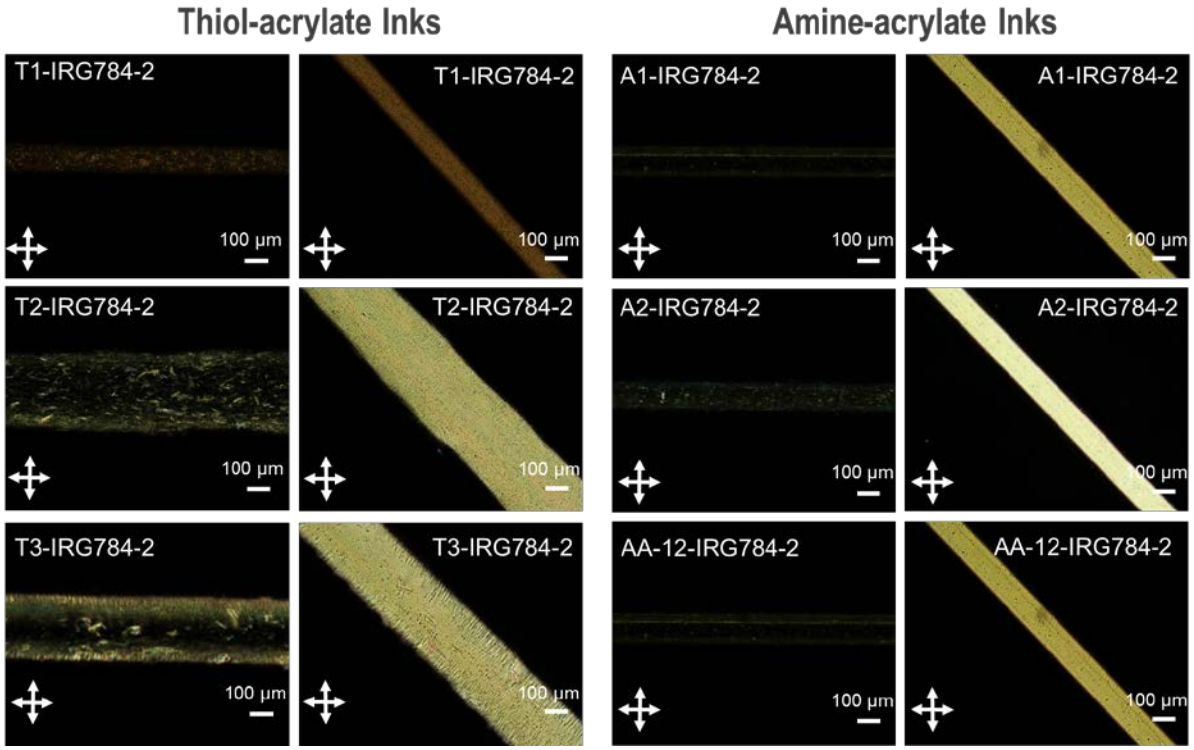

Figure 8, Polarized optical micrographs showing birefringence of a uniaxially printed polymer line at 0° (left) and 45° (right) to the polarizer for T1-IRG784-2, T2-IRG784-2 and T3-IRG784-2, A1-IRG784-2, A2-IRG784-2 and AA-12-IRG784-2.

PRIME has received Funding from the European Union's Horizon 2020 research and innovation programme under Grant Agreement No. 829010

3D printing of continuous stripes of liquid crystal elastomers (LCEs) with uniaxial orientation is obtained by printing closely packed parallel lines (typically 150 µm distance between lines) along one direction. Figure 9 shows scratch model of samples printed by using different inks. Figure 10 shows the observed birefringence of deposited ink between crossed polarizers for **T1-IRG784-2** ink. The resulting printed lines are subsequently fixed by photo-exposure (530 nm, using a green LED (Thorlabs M530L4) at 5 cm distance) for 1 h at room temperature. This photopolymerization leads to crosslinked elastomer formation. All printed samples presented the same anisotropic characteristics as the uncured ones when observed in the microscope. Aligned birefringent lines can be observed for the samples prepared in 1 week after ink preparation (as in Figure 10).

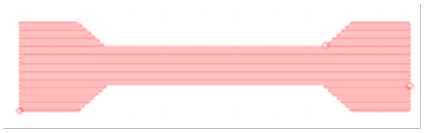

Figure 9, Schematic representation of LCE samples. The dog-bone model is consisting of continuous stripes of ink with uniaxial orientation. It contains closely packed parallel lines (150 µm) along one direction (long side).

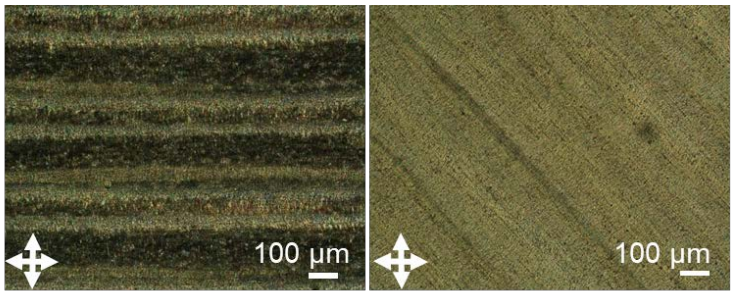

Figure 10, Polarized optical micrographs showing birefringence of a uniaxially printed LCE at 0° (left) and 45° (right) to the polarizer, immediately after printing the fresh ink.

The stability of the inks was also evaluated. Figure 11 shows a sample printed one month after the ink preparation. Poor alignment is observed using similar printing conditions for thiol-acrylate inks. This strongly suggests the use of prepared ink in a week after the oligomer is synthesized or the modification of the ink to prevent side-reactions and therefore achieve longer stability. To further investigate this point, the thiol-acrylate oligomers were dissolved in THF (Figure 12). Sample showing a turbid solution in THF indicates side-reactions, e.g. cross-linking, due to the presence of residual catalyst.

PRIME has received Funding from the European Union's Horizon 2020 research and innovation programme under Grant Agreement No. 829010

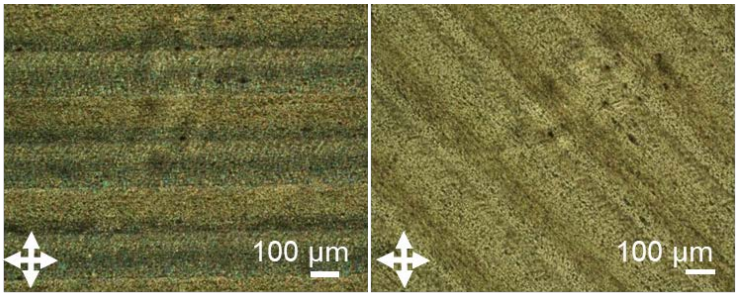

Figure 11, Polarized optical micrographs showing birefringence of a uniaxially printed LCE at 0° (left) and 45° (right) to the polarizer, printing one month after the ink preparation.

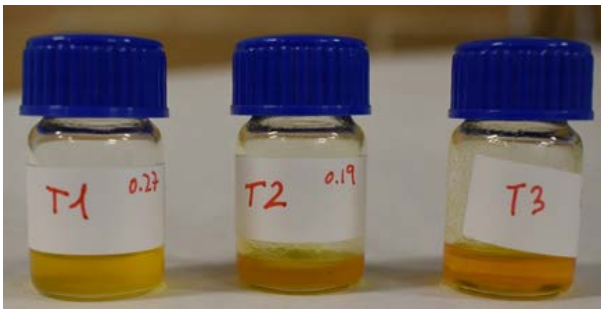

Figure 12, T1, T2 and T3 oligomers were dissolved in THF to observe the catalyst presence.

We restrict the results afterwards to the samples prepared with fresh ink in which a good alignment is obtained after printing and it is kept after photocuring. After printing and curing, samples that preserved the alignment are immersed in water that dissolves the PVA layer and the resulting LCEs structures are released. Once released from the substrate, samples are left to dry in room temperature overnight and stored to be used for thermo- and photoactuation studies.

In all cases except for **A1-IRG784-2**, the sample retained the original shape and size after drying process. Figure 13a shows an example for the initial shape of the LCE samples before immersing into water. However, samples of **A1-IRG784-2** ink have shrunken to a quarter of the initial size of the printed samples. Figure 13b-d show final shape and form of 3 different samples of **A1-IRG784-2** after left immersed in water for 24 h. We have repeated this step for different samples and the behaviour was consistent. While shape and size are stable for the rest of samples, those prepared with **A1-IRG784-2** present strong contraction when exposed to water, a phenomenon that might be related to a deficient LCE network formation as the structural characterization of the oligomer preparation has shown by TU/e. This precluded to perform further studies with this material.

PRIME has received Funding from the European Union's Horizon 2020 research and innovation programme under Grant Agreement No. 829010

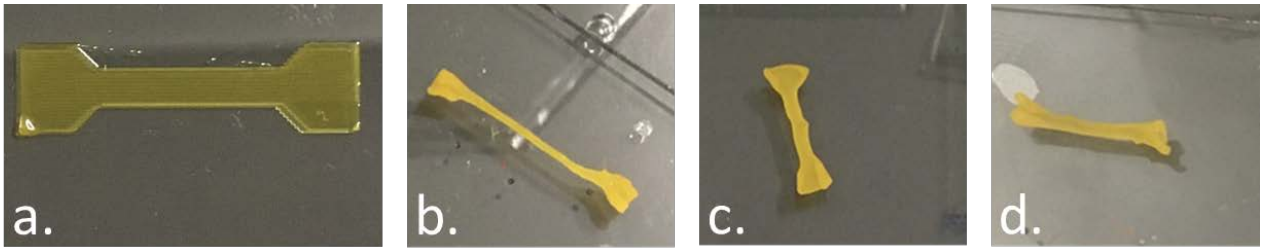

Figure 13, a) Image shows LCE samples after printing and curing on a glass substrate coated with PVA. b-d) Images show final shape and form of 3 different A1-IRG784-2 samples after immersed in water for 24 h.

5.2.3 Thermo-actuation of samples

To get insight into the mechanical response of the printed samples, thermo-actuation is studied by fixing the samples from one extreme and exposing them to different temperatures. The thermal response of **T1-IRG784-2**, **T2-IRG784-2**, **T3-IRG784-2**, **A2-IRG784-2**, and **AA-12-IRG784-2** is characterized by image analysis of the printed LCE structures exposed to temperatures from 30 ºC to 100 °C . Figure 14 showsan example for the thermal contraction along the printing direction of a LCE sheet made of T2-IRG784-2 by heating up to 100 ºC in an oven provided with an optical access.

Figure 15 shows changes in normalized length of different LCE stripes with temperature. In all cases, samples contract on heating, approximately half of their initial length, therefore showing an important mechanical response to external stimuli. Typically, LCE samples were cooled down to 40 ºC to relax back to their original size. All the stripes were relaxed back to their initial size except for samples prepared with **T1-IRG784-2** that did not restore the original size, a behaviour that could be ascribed to insufficient network formation.

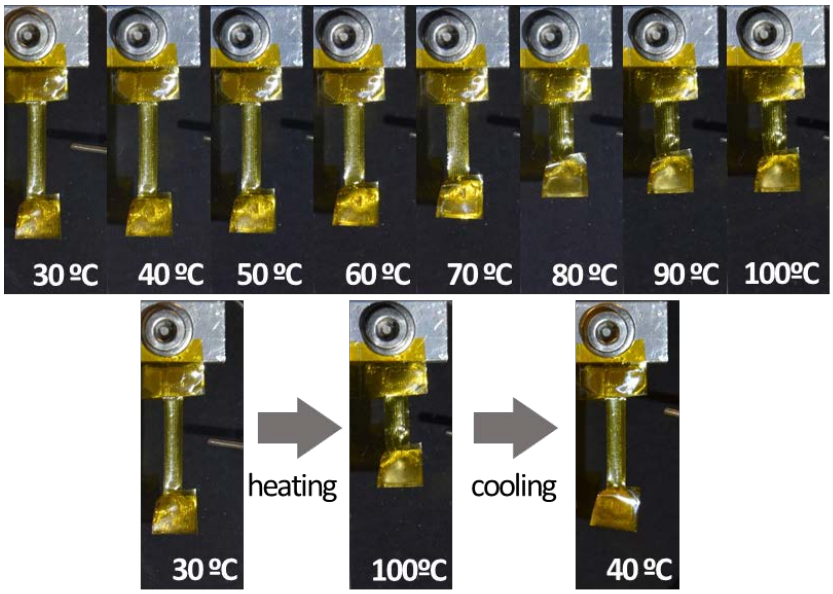

Figure 14, Top: Thermomechanical deformation of a free-standing sample. Sample printed having a shape of a dog bone. Bottom: Sample after heating to 100 ºC and its relaxation through cooling down to 30 ºC.

PRIME has received Funding from the European Union's Horizon 2020 research and innovation programme under Grant Agreement No. 829010

5.2.4 Photoactuation of samples

Photoactuation is also studied by acquiring images of the sample before UV exposure and later a sequence of images at different times during the irradiation. LCE sheet shape and dimensions have been evaluated, before and after exposed to UV light (50 mW/cm^2). The response to stimuli, contraction along the director and expansion along the perpendicular direction, is characterized by image analysis of the LCE sample at different illumination conditions.

For the sample made out of **T1-IRG784-2** ink, the initial length did not change after UV irradiation (Figure 16). Deficient network formation could be responsible for the lack of response in these materials. Differently, significant contraction upon UV irradiation was observed in other samples. Response times in the order of ten seconds were observed for these systems. Contractions up to 10% of the original length have been observed for samples made of thiol-acrylate based **T3-IRG784-2**. After the UV light has turned off, the sample recovered 95% of its initial length (Figure 17).

PRIME has received Funding from the European Union's Horizon 2020 research and innovation programme under Grant Agreement No. 829010

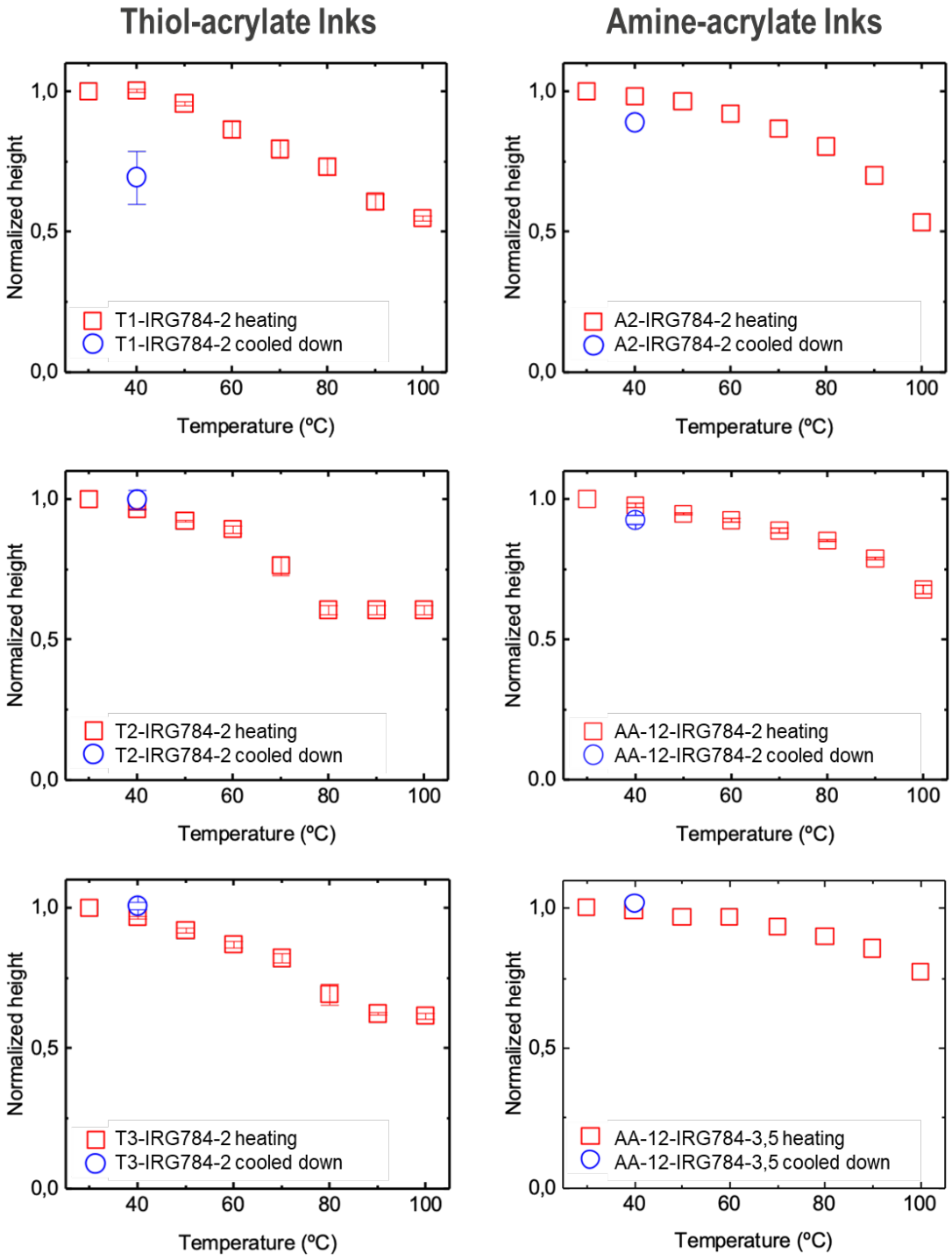

Figure 15, Normalized height versus temperature of a free-standing sample of thiol- and amine-acrylate based inks. Heating is shown as red squares and cooled down sample at 40 ºC is shown as blue circles.

PRIME has received Funding from the European Union's Horizon 2020 research and innovation programme under Grant Agreement No. 829010

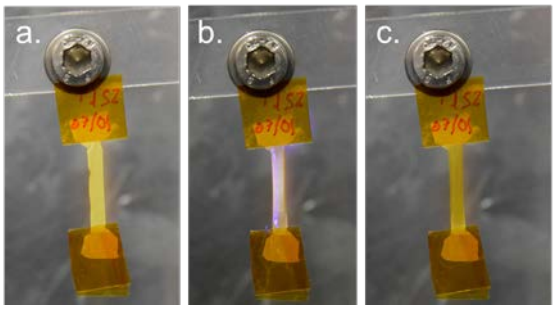

Figure 16, Photomechanical deformation of a free-standing dog-bone shaped LCE sheet of T1-IRG784-2 at a) t=0 before excitation; b) 10 min after UV irradiation of 50mW/cm^2 intensity; c) relaxation of the sample 2 min after UV has turned off.

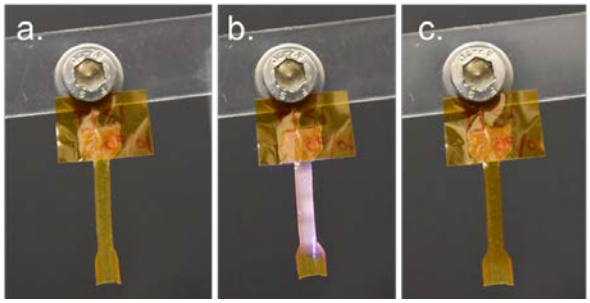

Figure 17, Photomechanical deformation of a free-standing dog-bone shaped LCE sheet of T3-IRG784-2 at a) t=0 before excitation; b) 10 min after UV irradiation of 50mW/cm^2 intensity; c) relaxation of the sample 2 min after UV has turned off.

5.2.5 Force characterization of samples

We explored the mechanical behaviour of LCE samples by measuring active tension in air on stimulation with a UV light source. Contraction of the LCE strips was activated with UV light illumination. After some irradiation period, once a stationary response was achieved, samples were then relaxed by switching the light source off.

To get a more quantitative characterization of the active mechanical photoresponse of the samples during the exposure to UV light, we have tried to quantify the involved forces. Figure 18 and 19 show the force measurements for different samples. Photoactuation studies of T1 ink, as shown in Figure 16, did not show any contraction along the director or expansion along the perpendicular direction and in this regime of UV light intensities either which might be related to a deficient network formation. In other cases, force was characterized as a function of UV intensity.

Figure 18 shows normalized force for thiol-acrylate exposed to different UV light intensities. The higher the energy applied; higher forces were obtained for all samples. These samples were heated slightly up to 35 ºC when illuminated with 50 mW/cm^2, however the sample heating was increased up to 70ºC when the illumination intensity was increased to 200 mW/cm^2.

Amine-acrylate systems have also been explored and the normalized forces were shown in Figure 19. Higher forces were obtained when the illumination intensity increased from 50 to 200 mW/cm^2. Different amounts of photoinitiator have been explored for **AA-12** with 2 and 3,5 wt.% of

PRIME has received Funding from the European Union's Horizon 2020 research and innovation programme under Grant Agreement No. 829010

IRGACURE 784. Results are suggesting that the larger photoinitiator content leads to significantly larger response. The origin of this behaviour is currently under study.

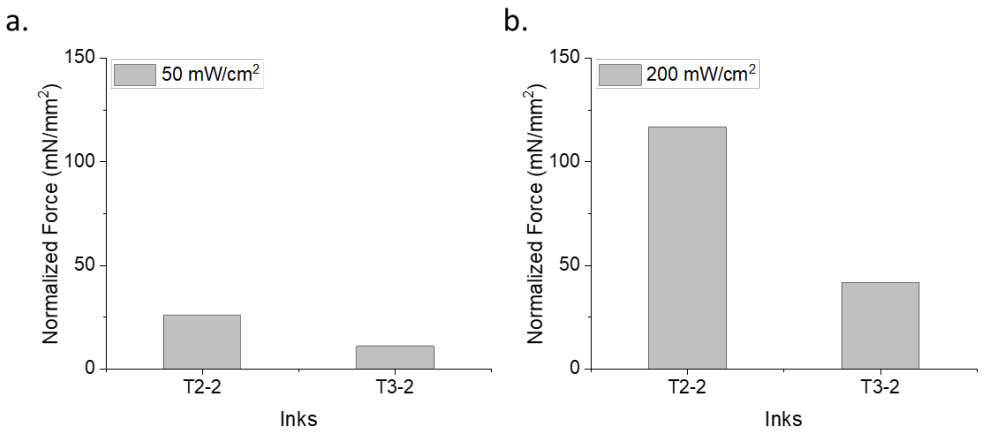

Figure 18, Normalized force measurements of thiol-acrylate samples T2-IRG784-2 (T2-2) and T3-IRG784-2 (T3-2) with UV irradiation of a) 50 mW/cm^2 and b) 200 mW/cm^2.

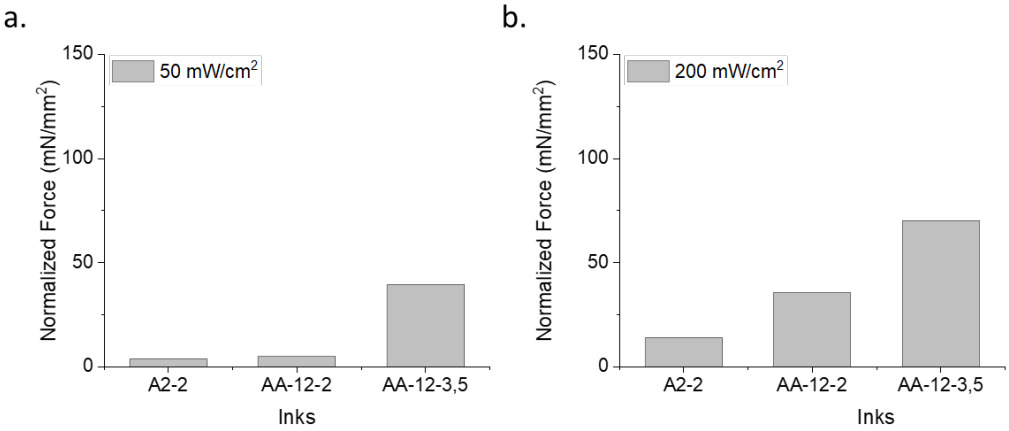

Figure 19, Normalized force measurements of amine-acrylate samples A2-IRG784-2 (A2-2), AA-12-IRG784-2 (AA-12-2) and AA-12-IRG784-3,5 (AA-12-3,5) with UV irradiation of a) 50 mW/cm^2 and b) 200 mW/cm^2

PRIME has received Funding from the European Union's Horizon 2020 research and innovation programme under Grant Agreement No. 829010

6 CONCLUSIONS

We have successfully prepared a first round of inks based on thiol- and amine- acrylate oligomers containing azobenzene moieties as photoresponsive units. Three different thiol-acrylate oligomers were prepared with different spacer length and regularity. By changing the spacers, the phase behaviour could be altered. Unfortunately, the inks based on thiol-acrylate oligomers have shown some instability issues upon longer storage. Using fresh inks within a week good results were obtained. But after longer storage, apparent cross-linking reactions occur. Also, two amine-acrylate oligomers were prepared having different molecular weights. However, the conditions for the aza-addition reaction were not optimal in all the cases, leading to lower molecular weight oligomers than was aimed for. This led a deficient LCE network of some amine-acrylate inks probably due to the uncomplete crosslinking after photopolymerization.

Overall, the 3D printed samples showed good alignment before and after UV curing. Thermo-actuation of the printed samples has been explored to get insight of the mechanical response and reversibility. Samples were typically contracted nearly half of their initial length after heating and relaxed back to their initial size after cooling down. LCE samples prepared with **T1** oligomer were not relaxed back to their initial size due to network formation issues in these samples. These samples were not contracted upon UV irradiation either. On contrary, for other samples, the photoactuation studies have shown contractions up to 10% by UV light within the order of ten seconds of response time. The force measurements have shown that normalized force increases when illumination intensities increases. The increase of photoinitiator amount in ink formation has demonstrated to increase the response to UV light in some of the materials.

7 OPEN POINTS AND OUTLOOK

For the next reporting period, a new set of oligomers will be prepared using optimized conditions. The molecular weight and the azo content will be varied to explore the effects of cross-link density and photo-thermal contributions. The results obtained will form the basis for modelling and integration of the materials in WP2.

To reduce photothermal contributions and eliminate using harmful UV-light, fluorinated azobenzene chromophores will be synthesized an incorporated. First experiments will be carried out using the monomer depicted in Figure 20. 500 mg of this monomer is already available for the first experiments.

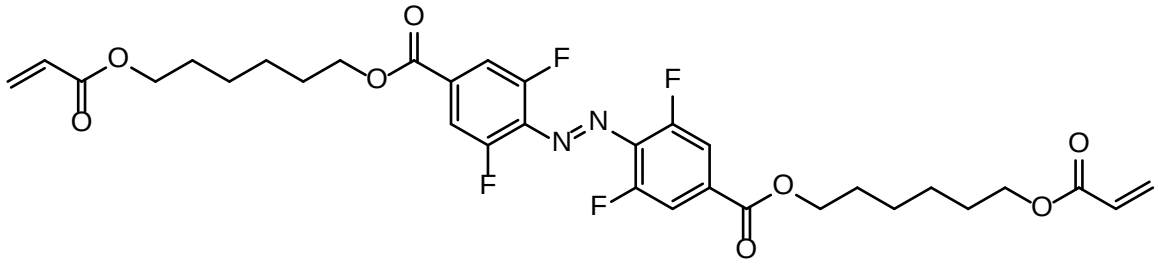

Figure 20, Fluorinated azobenzene derivate having a long *cis* lifetime.

Furthermore, new siloxane spacers have been designed and will be incorporated to lower the T_g and viscosity of the ink and elastomers (Figure 21). Dithiol **a** can be prepared in one singe

PRIME has received Funding from the European Union's Horizon 2020 research and innovation programme under Grant Agreement No. 829010

synthesis from low cost reagents. Primary amine **b** is commercially available and can directly be used.

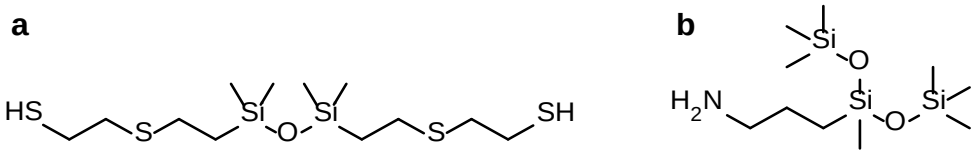

Figure 21, Siloxane dithiol and amine.

Lastly, thermoplastic LCEs will be evaluated either in their pure form or as semi-IPNs for 4D printing use and better processing and control over mechanical properties. The physical and mechanical properties of chemically crosslinked LCEs can sometimes be hard to predict and control which restricts the ability to optimize the material. Implementing reactive oligomers requires photocuring after each manufacturing step, e.g. 4D printing, which in general result in fixed structures that limit the recyclability and processability of the material. Moreover, photocuring is a time-consuming and energy-intensive process that slows down the additive manufacturing of actuator materials and affect the exposed structures thereof. Hence, a type of thermoplastic liquid crystal elastomers has been introduced which are melt-processable, de- and reformable, recyclable and has straightforward tunable mechanical properties.

For all these materials, the effect of 4D printing processing conditions will be optimized seeking for large and fast deformation and optimized work capacity when exposed to light. As in this first year, design of the materials together with its corresponding processing need to be done taking into account their integration in functional microfluidic devices.

PRIME has received Funding from the European Union's Horizon 2020 research and innovation programme under Grant Agreement No. 829010

8 REFERENCES

1. Kotikian, A., Truby, R. L., Boley, J. W., White, T. J. & Lewis, J. A. 3D Printing of Liquid Crystal Elastomeric Actuators with Spatially Programed Nematic Order. *Adv. Mater.* **30**, 1870063 (2018).
2. López-Valdeolivas, M., Liu, D., Broer, D. J. & Sánchez-Somolinos, C. 4D Printed Actuators with Soft-Robotic Functions. *Macromol. Rapid Commun.* **39**, 1700710 (2018).
3. Ambulo, C. P. *et al.* Four-dimensional Printing of Liquid Crystal Elastomers. *ACS Appl. Mater. Interfaces* **9**, 37332–37339 (2017).
4. Ula, S. W. *et al.* Liquid crystal elastomers: an introduction and review of emerging technologies. *Liq. Cryst. Rev.* **6**, 78–107 (2018).
5. Küpfer, J. & Finkelmann, H. Nematic liquid single crystal elastomers. *Die Makromol. Chemie, Rapid Commun.* **12**, 717–726 (1991).
6. Mukbaniani, O. *et al.* Formation of polymethylsiloxanes with alkyl side groups. *J. Appl. Polym. Sci.* **104**, 1176–1183 (2007).
7. Nair, D. P. *et al.* The Thiol-Michael addition click reaction: A powerful and widely used tool in materials chemistry. *Chem. Mater.* **26**, 724–744 (2014).
8. Kim, H., Boothby, J. M., Ramachandran, S., Lee, C. D. & Ware, T. H. Tough, Shape-Changing Materials: Crystallized Liquid Crystal Elastomers. *Macromolecules* **50**, 4267–4275 (2017).
9. Sánchez-Ferrer, A., Merekalov, A. & Finkelmann, H. Opto-Mechanical Effect in Photoactive Nematic Side-Chain Liquid-Crystalline Elastomers. *Macromol. Rapid Commun.* **32**, 671–678 (2011).
10. Finkelmann, H., Nishikawa, E., Pereira, G. G. & Warner, M. A new opto-mechanical effect in solids. *Phys. Rev. Lett.* **87**, 015501/1--015501/4 (2001).
11. Bisoyi, H. K. & Li, Q. Light-Driven Liquid Crystalline Materials: From Photo-Induced Phase Transitions and Property Modulations to Applications. *Chem. Rev.* **116**, 15089–15166 (2016).
12. Ikeda, T. & Ube, T. Photomobile polymer materials: From nano to macro. *Materials Today* **14**, 480–487 (2011).
13. Camacho-Lopez, M., Finkelmann, H., Palffy-Muhoray, P. & Shelley, M. Fast liquid-crystal elastomer swims into the dark. *Nat. Mater.* **3**, 307–310 (2004).
14. Yu, Y., Nakano, M., Shishido, A., Shiono, T. & Ikeda, T. Effect of Cross-linking Density on Photoinduced Bending Behavior of Oriented Liquid-Crystalline Network Films Containing Azobenzene. *Chem. Mater.* **16**, 1637–1643 (2004).
15. Yamada, M. *et al.* Photomobile polymer materials: Towards light-driven plastic motors. *Angew. Chemie - Int. Ed.* **47**, 4986–4988 (2008).
16. Iamsaard, S. *et al.* Fluorinated Azobenzenes for Shape-Persistent Liquid Crystal Polymer Networks. *Angew. Chemie - Int. Ed.* **55**, 9908–9912 (2016).
17. Gelebart, A. H., Mc Bride, M., Schenning, A. P. H. J., Bowman, C. N. & Broer, D. J. Photoresponsive Fiber Array: Toward Mimicking the Collective Motion of Cilia for Transport

PRIME has received Funding from the European Union's Horizon 2020 research and innovation programme under Grant Agreement No. 829010

Applications. *Adv. Funct. Mater.* **26**, 5322–5327 (2016).

18. Saed, M. O. *et al.* High strain actuation liquid crystal elastomers via modulation of mesophase structure. *Soft Matter* **13**, 7537–7547 (2017).
19. Gelebart, A. H., Mc Bride, M., Schenning, A. P. H. J., Bowman, C. N. & Broer, D. J. Photoresponsive Fiber Array: Toward Mimicking the Collective Motion of Cilia for Transport Applications. *Adv. Funct. Mater.* **26**, 5322–5327 (2016).
20. Chan, J. W., Hoyle, C. E., Lowe, A. B. & Bowman, M. Nucleophile-initiated thiol-michael reactions: Effect of organocatalyst, thiol, and Ene. *Macromolecules* **43**, 6381–6388 (2010).
21. Ware, T. H., McConney, M. E., Wie, J. J., Tondiglia, V. P. & White, T. J. Voxelated liquid crystal elastomers. *Science (80-.).* **347**, 982–984 (2015).
22. Desmet, G. B. *et al.* Quantitative First-Principles Kinetic Modeling of the Aza-Michael Addition to Acrylates in Polar Aprotic Solvents. *J. Org. Chem.* **81**, 12291–12302 (2016).

PRIME has received Funding from the European Union's Horizon 2020 research and innovation programme under Grant Agreement No. 829010